NATIONAL ADVISORY COMMITTEE FOR AERONAUTICS

REPORT No. 413

A METHOD FOR COMPUTING LEADING-EDGE LOADS

By RICHARD V. RHODE and HENRY A. PEARSON

1931

For sale by the Superintendent of Documents, Washington, D. C. - - - - - - - - - - - - - - Price 10 cents

AERONAUTICAL SYMBOLS

1. FUNDAMENTAL AND DERIVED UNITS

	Symbol	Metric		English	
		Unit	Symbol	Unit	Symbol
Length	l	meter	m	foot (or mile)	ft. (or mi.)
Time	t	second	s	second (or hour)	sec. (or hr.)
Force	F	weight of one kilogram	kg	weight of one pound	lb.
Power	P	kg/m/s		horsepower	hp
Speed		km/h	k. p. h.	mi./hr.	m. p. h.
		m/s	m. p. s.	ft./sec.	f. p. s.

2. GENERAL SYMBOLS, ETC.

W, Weight $= mg$

g, Standard acceleration of gravity $= 9.80665$ m/s^2 $= 32.1740$ ft./sec.^{2}

m, Mass $= \frac{W}{g}$

ρ, Density (mass per unit volume).

Standard density of dry air, 0.12497 (kg-m^{-4} s^2) at 15° C. and 760 mm $= 0.002378$ (lb.-ft.$^{-4}$ sec.^{2}).

Specific weight of "standard" air, 1.2255 kg/m^3 $= 0.07651$ lb./ft.^{3}.

mk^2, Moment of inertia (indicate axis of the radius of gyration k, by proper subscript).

S, Area.

S_w, Wing area, etc.

G, Gap.

b, Span.

c, Chord.

$\frac{b^2}{S}$, Aspect ratio.

μ, Coefficient of viscosity.

3. AERODYNAMICAL SYMBOLS

V, True air speed.

q, Dynamic (or impact) pressure $= \frac{1}{2}\rho V^2$.

L, Lift, absolute coefficient $C_L = \frac{L}{qS}$

D, Drag, absolute coefficient $C_D = \frac{D}{qS}$

D_o, Profile drag, absolute coefficient $C_{D_o} = \frac{D_o}{qS}$

D_i, Induced drag, absolute coefficient $C_{D_i} = \frac{D_i}{qS}$

D_p, Parasite drag, absolute coefficient $C_{D_p} = \frac{D_p}{qS}$

C, Cross-wind force, absolute coefficient $C_C = \frac{C}{qS}$

R, Resultant force.

i_w, Angle of setting of wings (relative to thrust line).

i_t, Angle of stabilizer setting (relative to thrust line).

Q, Resultant moment.

Ω, Resultant angular velocity.

$\rho\frac{Vl}{\mu}$, Reynolds Number, where l is a linear dimension.

e. g., for a model airfoil 3 in. chord, 100 mi./hr. normal pressure, at 15° C., the corresponding number is 234,000;

or for a model of 10 cm chord 40 m/s, the corresponding number is 274,000.

C_p, Center of pressure coefficient (ratio of distance of $c.\ p.$ from leading edge to chord length).

α, Angle of attack.

ϵ, Angle of downwash.

α_o, Angle of attack, infinite aspect ratio.

α_i, Angle of attack, induced.

α_a, Angle of attack, absolute.

(Measured from zero lift position.)

γ Flight path angle.

REPORT No. 413

A METHOD FOR COMPUTING LEADING-EDGE LOADS

By RICHARD V. RHODE and HENRY A. PEARSON
Langley Memorial Aeronautical Laboratory

93261—32

NATIONAL ADVISORY COMMITTEE FOR AERONAUTICS

NAVY BUILDING, WASHINGTON, D. C.

(An independent Government establishment, created by act of Congress approved March 3, 1915, for the supervision and direction of the scientific study of the problems of flight. Its membership was increased to 15 by act approved March 2, 1929 (Public, No. 908, 70th Congress). It consists of members who are appointed by the President, all of whom serve as such without compensation.)

JOSEPH S. AMES, Ph. D., *Chairman*,
President, Johns Hopkins University, Baltimore, Md.
DAVID W. TAYLOR, D. Eng., *Vice Chairman*,
Washington, D. C.
CHARLES G. ABBOT, Sc. D.,
Secretary, Smithsonian Institution, Washington, D. C.
GEORGE K. BURGESS, Sc. D.,
Director, Bureau of Standards, Washington, D. C.
ARTHUR B. COOK, Captain, United States Navy,
Assistant Chief, Bureau of Aeronautics, Navy Department, Washington, D. C.
WILLIAM F. DURAND, Ph. D.,
Professor Emeritus of Mechanical Engineering, Stanford University, California.
BENJAMIN D. FOULOIS, Major General, United States Army,
Chief of Air Corps, War Department, Washington, D. C.
HARRY F. GUGGENHEIM, M. A.,
The American Ambassador, Habana, Cuba.
CHARLES A. LINDBERGH, LL. D.,
New York City.
WILLIAM P. MACCRACKEN, Jr., Ph. B.,
Washington, D. C.
CHARLES F. MARVIN, M. E.,
Chief, United States Weather Bureau, Washington, D. C.
WILLIAM A. MOFFETT, Rear Admiral, United States Navy,
Chief, Bureau of Aeronautics, Navy Department, Washington, D. C.
HENRY C. PRATT, Brigadier General, United States Army,
Chief, Matériel Division, Air Corps, Wright Field, Dayton, Ohic.
EDWARD P. WARNER, M. S.,
Editor "Aviation," New York City.
ORVILLE WRIGHT, Sc. D.,
Dayton, Ohio.

GEORGE W. LEWIS, *Director of Aeronautical Research.*
JOHN F. VICTORY, *Secretary.*
HENRY J. E. REID, *Engineer in Charge, Langley Memorial Aeronautical Laboratory, Langley Field, Va.*
JOHN J. IDE, *Technical Assistant in Europe, Paris, France.*

EXECUTIVE COMMITTEE

JOSEPH S. AMES, *Chairman.*
DAVID W. TAYLOR, *Vice Chairman.*

CHARLES G. ABBOT.
GEORGE K. BURGESS.
ARTHUR B. COOK.
BENJAMIN D. FOULOIS.
CHARLES A. LINDBERGH.
WILLIAM P. MACCRACKEN, Jr.
CHARLES F. MARVIN.
WILLIAM A. MOFFETT.
HENRY C. PRATT.
EDWARD P. WARNER.
ORVILLE WRIGHT.

JOHN F. VICTORY, *Secretary.*

REPORT No. 413

A METHOD FOR COMPUTING LEADING-EDGE LOADS

By Richard V. Rhode and Henry A. Pearson

SUMMARY

In this report a formula is developed that enables the determination of the proper design load for the portion of the wing forward of the front spar. The formula is inherently rational in concept, as it takes into account the most important variables that affect the leading-edge load, although theoretical rigor has been sacrificed for simplicity and ease of application. Some empirical corrections, based on pressure distribuiion measurements on the "PW–9" and "M–3" airplanes, have been introduced to provide properly for biplanes.

Results from the formula check experimental values in a variety of cases with good accuracy in the critical loading conditions. The use of the method for design purposes is therefore felt to be justified and is recommended.

INTRODUCTION

Recent failures of the leading-edge structures of some airplanes at high angles of attack and in nose dives have indicated the necessity for a revision of the specifications for the design of the leading edge of the wing. (See figs. 1 and 2.) While the present Army and Navy design rules (references 1 and 2) furnish a fairly good criterion for the strength of the leading-edge structure in the high angle of attack condition, the entirely arbitrary provision for the nose-dive condition is inadequate in many cases. The Aeronautics Branch of the Department of Commerce has no rule for either case.

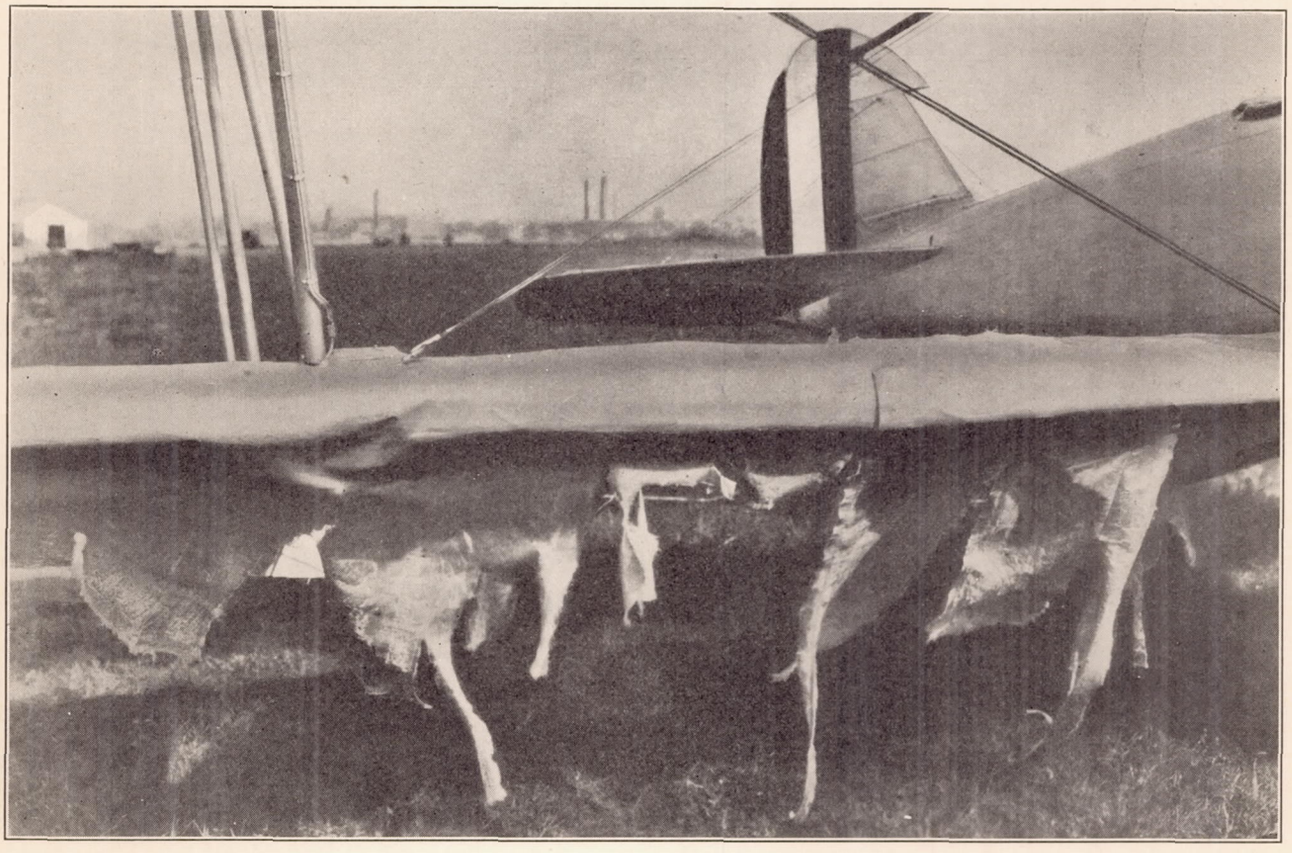

Figure 1.—Leading-edge failure that occurred in a fast dive

The National Advisory Committee for Aeronautics is now in a favorable position to study problems of this nature, making use of pressure-distrubution data from

flight tests and from tests at high Reynolds Numbers in the variable-density wind tunnel which have been accumulated over a period of years.

It is, therefore, the purpose of this paper to develop and to present a more satisfactory rule for the practical determination of leading-edge design loads than has heretofore existed.

The development of the formula involves, basically, theoretical considerations set forth in reference 3, although, in keeping with the interests of the practical designer, liberties have been taken with the rigorous theory to simplify the result as much as possible consistent with reasonable accuracy. Also, although the formula gives fair results for any condition of flight, it has been adjusted to give the best accuracy in the critical loading conditions.

The principal result sought has been the value of the shear at the forward face of the front spar. Thus, the formula is developed to obtain this result and does not include provisions for the rational determination of the moment. An examination of pressure diagrams, however, indicates that the centroid of the diagram area forward of the front spar, whatever the spar location, is confined within fairly narrow limits in terms of percentage of spar distance from the leading edge for all airfoils. Empirical rules for the location of the center of gravity of the leading-edge load are, therefore, derived from which a static test may be devised to give a reasonably correct value of the moment as well as the shear at the critical section.

DERIVATION OF THE FORMULA

In reference 3, Theodorsen shows that the total load on a wing section may be considered as the sum of a "basic" load, which is a function only of the shape of the mean camber line, and an additional load, which is a function of the angle of attack measured with respect to the "ideal" angle at which the basic load occurs and, to a minor extent, a function of the nose curvature. He shows, further, that the distribution of the basic load is a function of the mean camber, and that the distribution of the additional load is the same for any airfoil except for a narrow region near the leading edge where it becomes dependent upon the radius of the nose.

Figure 3 illustrates these points.

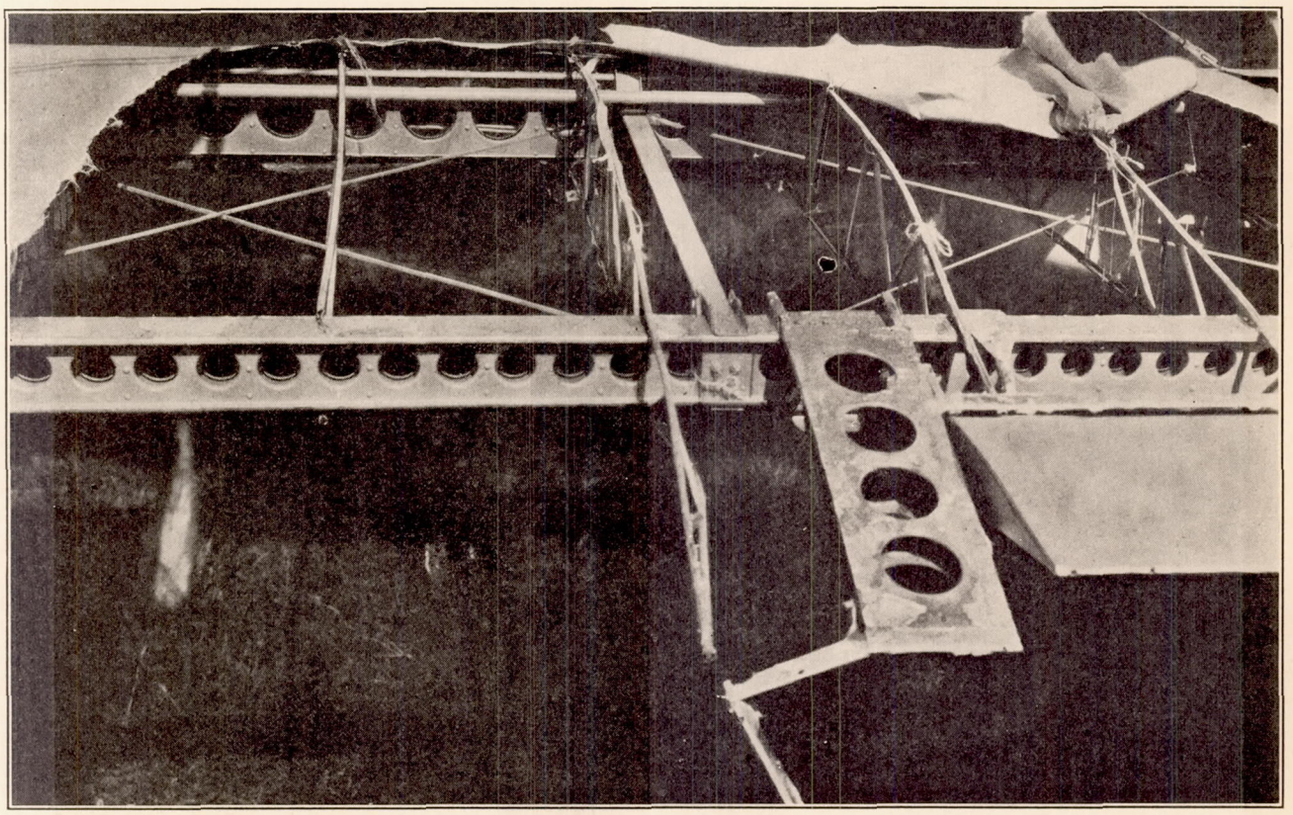

FIGURE 2.—Result of leading-edge failure. Air entering at the opening of the seam burst the fabric

Neglecting the minor variations at the nose, we may write, with only small error, for the whole wing section.

$$C_N = C_B + K\ (\alpha - \alpha_I) \tag{1}$$

where, C_N—total load coefficient
C_B—basic load coefficient at α_I
K—constant additional load per radian
α—nominal or geometric angle of attack (radians)
α_I—ideal angle of attack

For the present purpose it is of interest to examine the portion of the load forward of the front spar location, which is usually anywhere from 8 to 15 per cent of the chord. Equation (1) may be modified as follows:

$$C_S = k\ C_B + K'\ (\alpha - \alpha_I) \tag{2}$$

where, C_S is the load coefficient forward of front spar face and k and K' are appropriate constants.

Equation (2) is in such a form that the leading-edge load is given as a fraction of the total load on the section. The use of the function $(\alpha-\alpha_I)$ restricts the application of the formula to two-dimensional flow, and, for a practical case, the induced angle of attack α_i would have to be determined and subtracted from α. Further, α_I would have to be determined from the Gauss solution of Theodorsen's expression, viz:

$$\alpha_I{}^\circ = 6.23\ (y_1-y_5) + 0.47\ (y_2-y_4)$$

where y_1, y_2, y_4, and y_5 are the ordinates of the mean camber line, as fractions of the chord, with respect to a line joining the extremities of the mean camber line, at stations $x_1=0.00542\ c$, $x_2=0.125c$, $x_4=0.874\ c$, and $x_5=0.995\ c$.

The formula may be simplified and its use facilitated by the substitution of a function of C_N for $(\alpha-\alpha_I)$. Referring to Figure 4,

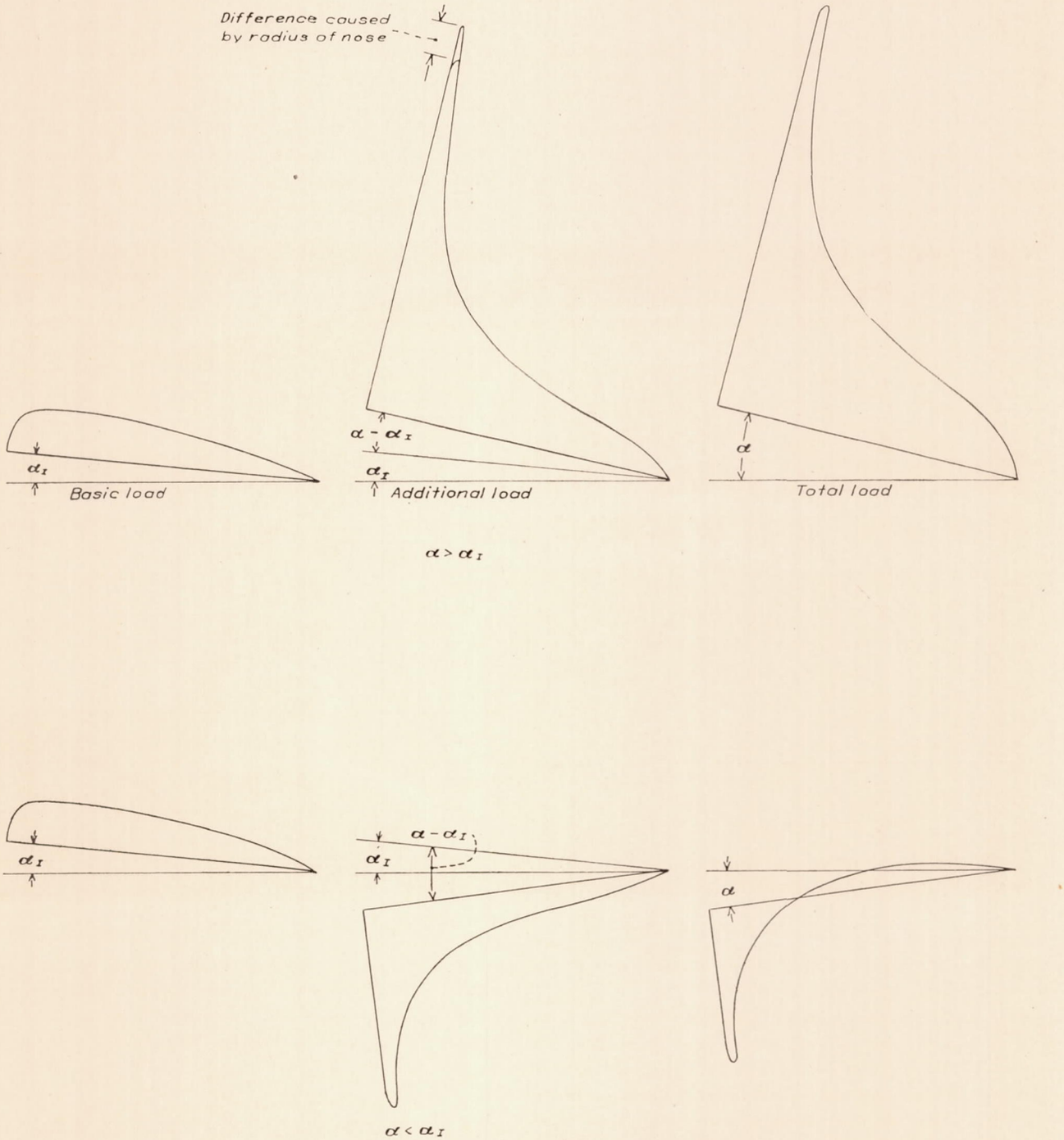

FIGURE 3.—Pressure distribution above and below the "ideal" angle of attack

$$(\alpha-\alpha_I)=\frac{C_N-C_B}{\frac{\Delta C_N}{\Delta\alpha}}$$

where, $\frac{\Delta C_N}{\Delta\alpha}=5.5$.

Substituting in equation (2), the following expression is obtained:

$$C_S=k\ C_B+K'\left(\frac{C_N-C_B}{5.5}\right) \tag{3}$$

At this point it is necessary to determine k, C_B, and K'. It has been pointed out that the distribution of the additional load which arises as a result of any departure from α_I is constant. The value of K', therefore, depends only upon the spar location, and graphical integration of the additional load-curve area forward of any particular front spar face yields the desired result. C_B is a function of the mean camber line and varies from zero for symmetrical sections to finite positive quantities for cambered airfoils. It may be considered negative for inverted sections. While its value may be determined precisely only by means of pressure measurements at the ideal angle of attack or by Theodorsen's expression, an approximation is sufficient for the present purpose. It may be said here, in justification of this step, that the ideal angle of attack is the angle at which the flow enters the leading edge smoothly, corresponding to the Kutta condition for smooth flow at the trailing edge. The basic load on the forward portion of the section is therefore small compared to the additional load imposed when the airfoil is at the angle of attack of maximum lift, one of the critical loading conditions for the leading edge. The same argument applies for the other critical condition, that of nose dive, in which, for commonly used airfoils, the value of $\alpha-\alpha_I$ is also large. The argument does not apply to airfoils with very low camber near zero lift, but in such cases the total loads are small and of little interest. It is, therefore, assumed, for the sake of simplicity, that the value of C_B is a function only of the general shape of the median line and of the maximum mean camber (measured always with respect to the chord of the mean camber line), and that the value of k, which is the portion of the basic load forward of the spar, is a function only of spar location for airfoils of the same general shape. To obtain working values of C_B and k, curves have been drawn through theoretically derived values for several airfoils of conventional and reflex form with various cambers and, in the case of k, for several spar locations.

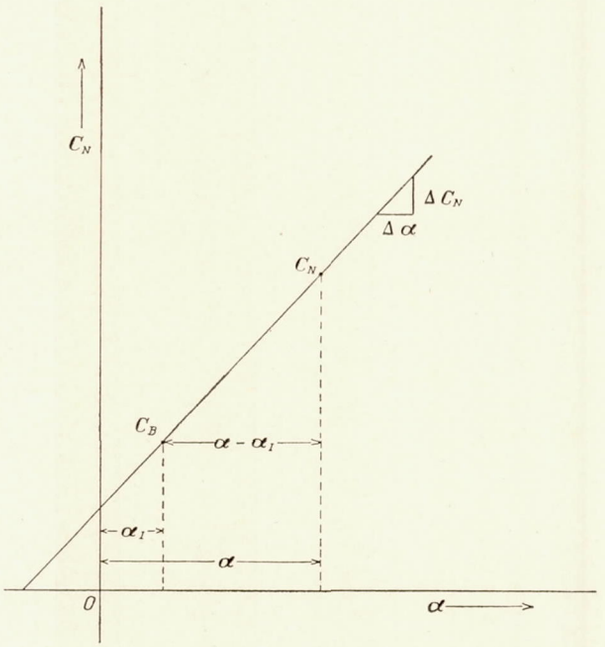

FIGURE 4.—Relation between C_N and C_B

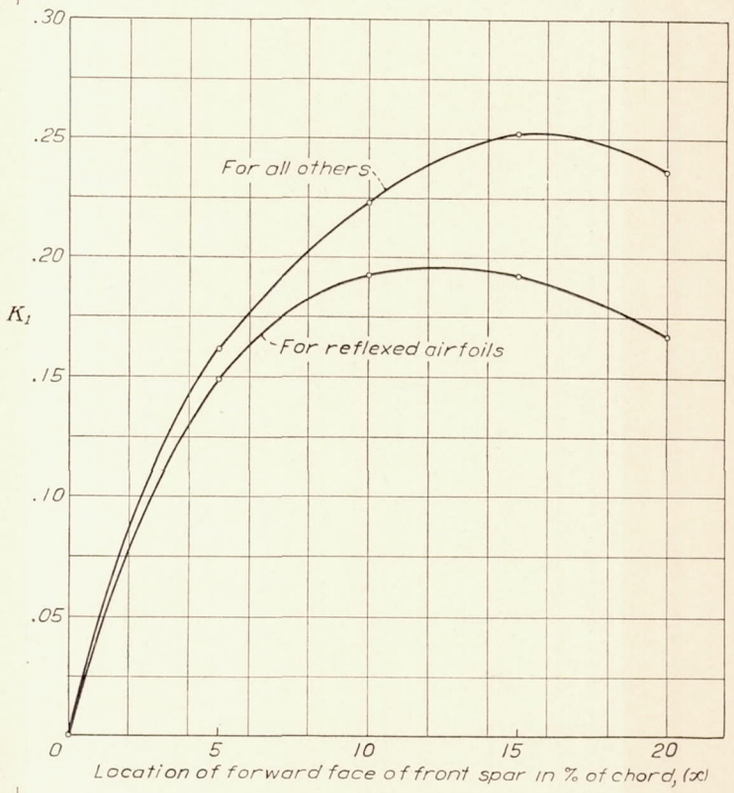

FIGURE 5.—K_1 against spar location

Before the formula is put in its final form, the normal discrepancy between theoretical and experimental results must be taken into account. This discrepancy arises largely as a result of skin friction and is evidenced by progressively increasing pressure losses as the trailing edge is approached. The effect is, therefore, to shift the line of action of the experimental total load forward of that for the theoretical load, which results in an increase in the values of k and K'. The multiplying factor for k and K' was found, by a method of averages, to be 1.17.

The formula may now be written

$$C_S=1.17\left(k-\frac{K'}{5.5}\right)C_B+\frac{1.17\ K'C_N}{5.5} \tag{4}$$

The result is further condensed to

$$C_S = (-K_1 C_B + K_2 C_N) \qquad (5)$$

which is the final and useful form, giving what may be termed the "leading-edge shear coefficient," or the leading-edge load per unit chord, per unit span, per unit q. From this, substituting C_L for C_N, the total load per unit span is

$$w_{l.e.} = C_S \tfrac{1}{2}\rho V^2 c$$
$$= (-K_1 C_B + K_2 C_L) c \times \tfrac{1}{2}\rho V^2)$$

where c, ρ, and V have their usual significance.

Curves for K_1 and K_2 as functions of spar location are given in Figures 5 and 6, respectively, and curves of

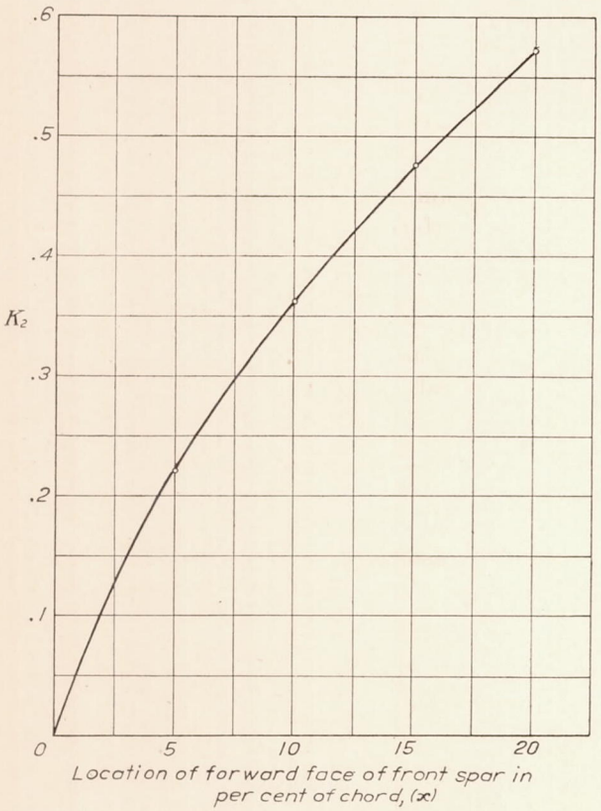

FIGURE 6.—K_2 against spar location

C_B against maximum mean camber are given in Figure 7. Figure 8 is included merely to show the manner in which y_{max} is measured.

COMPARISON OF RESULTS FROM FORMULA AND FROM PRESSURE-DISTRIBUTION TESTS

For the purpose of checking the validity of the formula by comparison with pressure-distribution diagrams, only those diagrams which were obtained from the variable-density wind tunnel at high Reynolds Numbers (reference 4) and from flight tests are used. While a vast quantity of pressure-distribution data from other sources is available, they have shown such inconsistency among themselves and with variable-density wind tunnel and flight results that it is believed advisable to avoid confusion, and possibly misleading conclusions, by the elimination of them from consideration altogether.

A comparison of the calculated shear coefficients C_S with experimental values obtained from tests on monoplane airfoils in the variable-density tunnel is given in Table I. It will be noted that the agreement is good at high angles of attack for the variety of airfoils and spar locations given, the maximum difference being 12.9 per cent in the case of the N. A. C. A. 84–J airfoil with spar location at 20 per cent chord.

At lift coefficients of zero or slightly below, representing the nose-dive condition, the agreement is quite good at all spar locations for the R. A. F. 30 and N. A. C. A. 84 airfoils. Larger errors, however, are apparent for

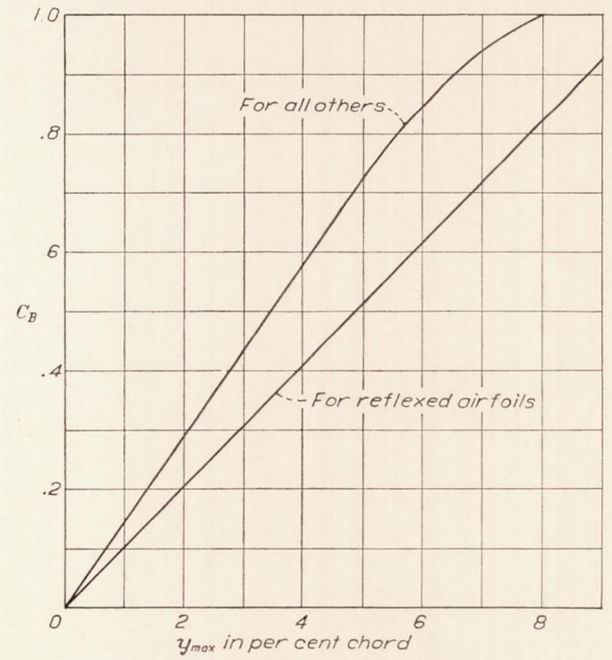

FIGURE 7.—Relation of C_B to maximum mean camber

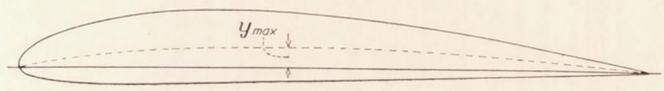

FIGURE 8.—Maximum mean camber, y_{max} of the Clark Y airfoil

the M–6, Clark Y, and 84–J. There are several reasons for this apparent decrease in accuracy. First, differential normal pressures are less at the nose near zero lift than at maximum lift when the air speed is maintained constant. This condition results in larger percentage experimental errors at the low angles of attack, since small pressures are more difficult to measure with accuracy than large pressures. Second, the peculiar shape of the pressure diagram for lift coefficients near zero is of itself a cause for greater experimental error. Slight inaccuracies in locating pressure orifices result in large percentage errors in the leading-edge shear coefficient since the pressure gradient along the chord near normal front-spar locations is extremely steep. This source of error is an important consideration when using test data from small models. In

addition, since the leading-edge part of the pressure diagram is roughly a narrow triangle in shape (see fig. 3), much depends upon the proper location of orifices and upon accurate measurement at a pressure station near the apex of the "triangle." Such causes as the above could easily explain most of the apparent 20 per cent error in the results on the Clark Y.

In the case of the M–6 another source of error exists. Because this airfoil has such a low camber, the value of $\alpha - \alpha_I$ is small near zero lift; thus the basic load, which in the formula is only approximated, largely predominates. In fact, it may be expected that, as $\alpha - \alpha_I$ approaches such a value that the difference between the "basic" pressures and the "additional" pressures near the nose approach zero, percentage errors will become infinitely great. These errors, however, have no practical significance. It is to be noted, in this connection, that the nose-dive shear coefficients for the M–6 are quite small compared with those for the other airfoils, excepting the symmetrical R. A. F. 30 section.

The greatest errors occur in the case of the N. A. C. A. 84–J airfoil slightly below zero lift. Pressure diagrams for this condition, showing definitely that the lower surface has stalled, indicate that these errors are almost entirely a result of the abnormal shape, or mean camber, of the section. It will be noted that the error is almost entirely eliminated if the concavity in the lower surface is removed to prevent this stalling; e. g., it will be noted that the error is small in the case of the N. A. C. A. 84, which is simply the 84–J with the concave lower surface replaced by a flat lower surface.

In view of the above discussion, the accuracy of the results obtained with the formula applied to monoplanes is considered reasonably good. It is to be doubted that better results could have been obtained without greater precision in test measurements and appreciably greater complications in the method or formula.

In Table II results obtained with the formula are compared with experimental results obtained in flight on the *M–3* and *PW–9* airplanes having the Clark Y and Göttingen 436 sections, respectively. The test data represented in this table are of an appreciably higher order of accuracy than those in Table I, having been recently obtained after improvements in test methods were effected. The maximum error on the Clark Y in this table is −11 per cent, an amount which is not greater than might be expected as a result of the biplane arrangement. The upper wing in this case is alone represented.

The error on the upper wing of the *PW–9* airplane is about the same in magnitude and of the same sign as the error on the *M–3* upper wing in the high angle of attack condition. In the nose-dive condition on the *PW–9* lower wing, however, the error is consistently high, averaging about 30 per cent, while on the upper wing in this condition the error is negligible.

EFFECT OF BIPLANE ARRANGEMENT

No attempt is made here to include rationally the effects of superposed wings as in biplane combinations. The character of these effects should, however, be understood and some provision made for them in the design.

One airfoil mounted beneath another airfoil may be considered to have two effects on the latter. First, by virtue of its downwash at positive values of lift, the lower wing causes the upper wing to operate at an effective angle of attack which is smaller than that at which it would operate as a monoplane. This effect does not influence appreciably the shape of the pressure diagram. Second, by virtue of the camber of the upper surface of the lower wing, the streamlines are curved even at an appreciable distance from the wing, a phenomenon which results in a decrease in the effective camber of the upper wing. This effect causes a small forward shift of the center of pressure on the upper wing at high angles of attack and an increase in the leading-edge load. Thus, it is to be expected that the formula for leading-edge loads will give low values for the upper wing at high angles of attack. On the *M–3* and *PW–9* airplanes (Table II) the result is 11 per cent too low. Most of this error, however, may be experimental error and error from the formula. In view of this and the reasonably small magnitude of the error, it is not considered necessary nor advisable to make any correction for the upper wing at high angles of attack.

The effect of the upper wing on the lower is likewise small at the high angles of attack.

At or near zero lift the effect of the curvature of the streamlines appears to be small on the upper wings of both the *M–3* and *PW–9*. On the *PW–9* lower wing, however, the effect appears to be quite pronounced, as has been previously shown. A number of careful tests near zero lift on this airplane all bear out the fact that the shear coefficient on the lower wing is about 30 per cent greater than that on the upper wing or that obtained from the formula. It is interesting to recall, in this connection, that the leading-edge failure on a recently built diving bomber occurred on the lower wing in a dive. (Figs. 1 and 2.) This evidence, with the results of the *PW–9* tests, indicates that the requirements for the lower wing of a biplane in the nose-dive condition should be increased over those for the upper wing or the monoplane. On the basis of the *PW–9* tests, it is suggested that this increase should be 30 per cent in some cases. Since the effect is probably caused by an induced change in camber resulting from curved air flow, it is more logical to include the effect in the formula by increasing the value of C_B rather than by increasing the final result arbitrarily by 30 per cent. From the *PW–9* tests it appears that the value of C_B should be increased 40 per cent for the biplane lower wing in the nose-dive condition. This

correction is recommended for general use until more information is available.

USE OF THE FORMULA

In any design, the strength of the leading edge should be investigated for the two critical conditions, (a) high angle of attack, and (b) nose dive. Experience, as well as analysis, has shown that no other condition need be considered and that in some cases, such as designs making use of symmetrical or nearly symmetrical airfoils and designs of large airplanes that are never dived, the high angle of attack condition only is of interest. To make use of the formula for these conditions, the leading-edge shear coefficient C_S, and the dynamic pressure $\frac{1}{2}\rho V^2$ must be known. C_S, as has been shown, is a function of the shape of the airfoil and of the value of C_N corresponding to the condition being investigated. In a given design, with the airfoil and spar locations known, the constants K_1, K_2, and C_B are readily determined from the curves given in Figures 5, 6, and 7. It is necessary to determine the values of C_N and $\frac{1}{2}\rho V^2$ that will make the strength of the leading edge consistent with the strength of the rest of the wing structure. This may be done as follows:

Case I—High angle of attack.—The primary wing structure is designed to fail in a condition corresponding to maximum C_N with a certain specified load factor. From the general lift equation, this is equivalent to saying,

$$nW = C_{N_{\max}} S \times \tfrac{1}{2} \rho_0 V_i^2$$

where, nW—the load at failure
n—high angle of attack load factor
W—weight
S—wing area
ρ_0—standard sea-level density
V_i—the indicated speed at which, with $C_{N_{\max}}$, the equation is satisfied

This speed V_i is the speed to use in the leading-edge formula for the high angle of attack condition, and $C_{N_{\max}}$ the proper value of C_N. It is not essential that $C_{N_{\max}}$ be determined with great precision, as any errors introduced in the shear coefficient will be approximately compensated by errors of opposite sense in V_i^2, with a resultant small error in the total leading-edge load. A representative problem, using the Clark Y airfoil, has indicated that $C_{N_{\max}}$ may be in error by as much as 25 per cent and cause only a 5 per cent error in the total leading-edge load.

In the case of biplanes, proper account should be taken of the relative wing-loading ratio. The above discussion of $C_{N_{\max}}$ applies strictly only to monoplanes. It applies to biplanes when $C_{N_{\max}}$ is considered as that for the cellule and is used to determine V_i^2. The mean lift coefficient for the biplane cellule should not be used in the formula to determine the leading-edge load for either upper or lower wings without correcting for the relative wing-loading ratio. This may be done by means of the following simple expressions, the wing-loading ratio being assumed known:

$$L_u + L_l = Wn$$

or,

$$L_u = Wn - L_l$$

where, L_u—lift on upper wing
L_l—lift on lower wing
W—gross weight
n—H. A. A. load factor

Also,

$$R = \frac{C_N \text{ (upper)}}{C_N \text{ (lower)}} = \frac{L_u}{L_l} \times \frac{S_l}{S_u} = \frac{Wn - L_l}{L_l} \times \frac{S_l}{S_u}$$

Solve the above equation for L_l. Then,

$$C_N \text{ (lower)} = \frac{L_l}{\frac{1}{2} \rho_0 V_i^2 S_l}$$

and C_N (upper) $= R \times C_N$ (lower) where V_i^2 is the value found using the cellule $C_{N_{\max}}$ and the high angle of attack load factor.

As in the case of the monoplane, the biplane-wing lift coefficients found by the above method may not be true values, since they depend on V_i^2, which itself has been found from an approximate cellule $C_{N_{\max}}$. However, this makes no practical difference, any errors resulting in the shear coefficient being compensated by an error of opposite sense in V_i^2 to give a substantially correct leading-edge design load.

The above biplane correction has nothing to do with the biplane corrections to the shear coefficient discussed in the preceding sections and is used merely to determine the proper values of C_N for the individual wings.

Corrections to allow for the variation of C_N along the span are not believed to be advisable in view of the added complication which would be involved.

Case II—Nose dive.—In the nose-dive condition, the terminal velocity or the limited diving speed should be determined. The value of C_N may be found by a solution of the conditions of static equilibrium for the case under consideration. It is suggested that, for the terminal-velocity dive, allowance be made for the possibility of encountering gusts and for slight inadvertent motions of the controls which may result in negative lift coefficients. This provision is important because the variation of leading-edge load with angle of attack near zero lift is extremely rapid, the load increasing greatly with small negative increments of lift coefficient. So little is known about atmospheric conditions that it is difficult to establish a criterion for the determination of the proper negative lift coefficients on the basis of gusts. An examination of pilot-balloon data taken at Langley Field over a period of three months indicates that variations in horizontal wind velocities may be assumed as 15 feet per second, which would result in negative lift coefficients of from -0.15 to -0.26 in the average case, depending on the terminal velocity. Other evidence exists which indicates

that a value of 15 feet per second is not too conservative. In addition to the possibilities of encountering gusts, there is also the fact that wings twist in dives under the heavy torsional moments experienced with the common wing sections. This influence may result in negative lift coefficients at the outer portion of the wing, even when the total lift coefficient is positive. Since this effect increases with speed, it is probably better to assume a constant negative lift coefficient for all cases instead of one which would vary approximately inversely with the speed if a standard gust were used as a basis. Until more is known about conditions in the dive, it is felt that a value of C_N not less than -0.2 should be used in the nose-dive analysis.

The correction for relative wing-loading ratio is not to be used for the nose-dive analysis, but the 40 per cent increase in C_B for the lower wings of biplanes, as recommended in the preceding section, should not be forgotten.

TYPICAL PROBLEM

Given:

Airplane	Biplane pursuit
Weight	2,720 pounds
Area (upper)	184 square feet
Area (lower)	88 square feet
Area (total)	272 square feet
Mean chord (upper)	5.75 feet
Mean chord (lower)	4.00 feet
Airfoil:	Clark Y
($y_{max}=3.60$ per cent; see fig. 6.)	
H. A. A. load factor n	12
Spar-face location x	10 per cent chord
Relative wing-load ratio	1.2
Terminal velocity	280 m. p. h. (410 f. p. s.) assumed

Required:

Shear at spar face on both upper and lower wings in

(*a*) H. A. A. condition

(*b*) N. D. condition

Solution:

Constants:

$K_1=0.223$

$K_2=0.367$

$C_B=0.525$

High angle of attack condition:

$C_{N\max}$(cellule) $=1.4$ (assumed)

$$V_i^2=\frac{2nW}{1.4S\rho_0}$$

$$=\frac{2\times12\times2{,}720}{1.4\times272\times0.002378}=72{,}100 \text{ (f. p. s.)}^2$$

$$R=\frac{nW-L_l}{L_l}\times\frac{S_l}{S_u}$$

or $$L_l=\frac{nW}{\left(R\frac{S_u}{S_l}+1\right)}=\frac{12\times2{,}720}{\left(1.2\times\frac{184}{88}+1\right)}=9{,}300 \text{ pounds}$$

$$C_{N_l}=\frac{9{,}300}{\frac{1}{2}\rho_0 V_i^2 S_l}=\frac{9{,}300}{85.7\times88}=1.23$$

and, $C_{N_u}=1.2\times1.23=1.48$.

Thus, for the *upper wing:*

$$w_{l.e.}=(-K_1C_B+K_2C_N)\frac{\rho_0}{2}V_i^2c_u$$

$$=(-0.223\times0.525+0.367\times1.48)\frac{0.002378}{2}\times72{,}100\times5.75$$

$=210$ pounds per foot span, or

$$\frac{210}{0.1\times5.75}=365 \text{ pounds per square foot average.}$$

For the *lower wing:*

$$w_{l.e.}=(-0.223\times0.525+0.367\times1.23)\frac{0.002378}{2}\times72{,}100\times4$$

$=118$ pounds per foot span, or

$$\frac{118}{0.1\times4}=295 \text{ pounds per square foot average.}$$

The preceding values are the total *design* loads.

Nose dive condition:

$K_1=0.223$, $K_2=0.367$, $C_B=0.525$ } as before

$C_{N_u}=-0.200$, $C_{N_l}=-0.200$ } assumed for N. D.

C_B (corrected for lower wing) $=1.4\times0.525=0.735$

Thus, for the upper wing:

$$w_{l.e.}=(-0.223\times0.525-0.367\times0.200)\frac{0.002378}{2}\times(410)^2\times5.75$$

$=219$ pounds per foot span.

For the lower wing:

$$w_{l.e.}=(-0.223\times0.735-0.367\times0.200)\frac{0.002378}{2}\times(410)^2\times4$$

$=190$ pounds per foot span.

The above values are the total *applied* loads. The design load is obtained by multiplying by a factor of safety, say 2, which gives a result of 438 pounds per foot for the upper wing and 380 pounds per foot for the lower wing.

It will be noted that it was not necessary to multiply the high angle-of-attack results by two, since the factor of safety was taken into account by using the *design* load factor in the determination of V_i^2. The same result would have been obtained by calculating V_i^2 on the basis of the expected maximum *applied* load factor or $n/2$ (in this case, 6) and multiplying the final result by the factor of safety, 2.

APPLICATION IN STATIC TESTS

It is desirable, in static tests of the leading edge, to use a rectangular load distribution. Such a distribu-

tion is permissible if the stresses imposed at the critical section in flight can be well represented in this way. If the rectangular load distribution is to be used, the moment at the critical section (always the forward face of the spar) must, in addition to the shear, be approximately correct.

No attempt has been made here to rationalize the determination of the moment of the leading-edge load about the face of the spar, since an empirical solution is believed to be within the limits of precision of practical static tests. It has been found, from an examination of a large number of pressure diagrams, that the location of the centroid of the part of the area forward of the front spar is, on the average, at 45 per cent of the spar location (0.45 x) in the high angle of attack condition, and at 35 per cent (0.35 x) in the nose-dive condition. The relative position varies slightly with different spar locations and with different airfoils, but within the usual range the variation amounts to not more than three-fourths of 1 per cent of the total chord or only a small fraction of an inch for the ordinary airplane.

Static tests may, therefore, be made using a rectangular load distribution, the center of gravity of the load being at,

0.45 x for H. A. A.
0.35 x for N. D.

LANGLEY MEMORIAL AERONAUTICAL LABORATORY,
NATIONAL ADVISORY COMMITTEE FOR AERONAUTICS,
LANGLEY FIELD, VA., *January 16, 1931.*

REFERENCES

1. Handbook of Instructions for Airplane Designers. Engineering Division, Army Air Service. (1931.)
2. Instructions for Testing of Airplane Structures. Navy Specification SR–9.
3. Theodorsen, Theodore: On the Theory of Wing Sections with Particular Reference to the Lift Distribution. T. R. No. 383, N. A. C. A., 1931.
4. Jacobs, Eastman N., Stack, John, and Pinkerton, Robert M: Airfoil Pressure Distribution Investigation in the Variable-Density Wind Tunnel. T. R. No. 353, N. A. C. A., 1930.

TABLE I

COMPARISON OF SHEAR COEFFICIENTS FROM FORMULA AND FROM PRESSURE-DISTRIBUTION TESTS IN THE VARIABLE-DENSITY TUNNEL

R. A. F.–30 AIRFOIL

Maximum mean camber=0% c; C_B=0

Spar location (% c)	C_L	K_1 (from curve)	K_2 (from curve)	C_S		Error, %	Remarks
				Computed	Experimental		
5	±1.20	0.162	0.222	0.266	0.253	5.1	H. A. A. condition.
	±.95	.162	.222	.211	.224	−5.8	
	±.76	.162	.222	.169	.176	−4.0	
	±.57	.162	.222	.127	.117	8.5	
	±.34	.162	.222	.0755	.074	2.0	
10	±1.20	.223	.361	.433	.443	−2.3	H. A. A. condition.
	±.95	.223	.361	.343	.376	−8.8	
	±.76	.223	.361	.274	.294	−6.8	
	±.57	.223	.361	.206	.204	1.0	
	±.34	.223	.361	.123	.129	−4.7	
15	±1.20	.252	.477	.572	.589	−2.9	H. A. A. condition.
	±.95	.252	.477	.453	.486	−6.8	
	±.76	.252	.477	.363	.385	−5.7	
	±.57	.252	.477	.272	.264	3.0	
	±.34	.252	.477	.162	.171	−5.3	
20	±1.20	.236	.571	.685	.702	−2.4	H. A. A. condition.
	±.95	.236	.571	.543	.577	−5.9	
	±.76	.236	.571	.434	.453	−4.2	
	±.57	.236	.571	.326	.315	3.5	
	±.34	.236	.571	.194	.208	−6.7	

N. A. C. A. M–6 AIRFOIL

Maximum mean camber=2.215% c; C_B=0.226

Spar location (% c)	C_L	K_1 (from curve)	K_2 (from curve)	C_S		Error, %	Remarks
				Computed	Experimental		
5	1.08	0.149	0.222	0.206	0.191	7.9	H. A. A. condition.
	1.05	.149	.222	.199	.203	−2.0	
	−.10	.149	.222	−.0559	−.0639	−12.5	Approximately N. D. condition.
10	1.08	.192	.361	.347	.337	3.0	H. A. A. condition.
	1.05	.192	.361	.336	.345	−2.6	
	−.10	.192	.361	−.0795	−.0808	−1.6	Approximately N. D. condition.
15	1.08	.192	.477	.472	.448	5.4	H. A. A. condition.
	1.05	.192	.477	.458	.459	−.2	
	−.10	.192	.477	−.0911	−.0833	9.4	Approximately N. D. condition.
20	1.08	167	.571	.579	.541	7.0	H. A. A. condition.
	1.05	.167	.571	.562	.559	.5	
	−.10	.167	.571	−.0948	−.0782	21.2	Approximately N. D. condition.

TABLE I—Continued

COMPARISON OF SHEAR COEFFICIENTS FROM FORMULA AND FROM PRESSURE-DISTRIBUTION TESTS IN THE VARIABLE-DENSITY TUNNEL—Con.

CLARK Y AIRFOIL

Maximum mean camber=3.6% c; $C_B = 0.525$

Spar location (% c)	C_L	K_1 (from curve)	K_2 (from curve)	C_S Computed	C_S Experimental	Error, %	Remarks
5	1.49	0.162	0.222	0.246	0.247	−0.4	H. A. A. condition.
	1.44	.162	.222	.235	.209	12.4	H. A. A. condition.
	.02	.162	.222	−.0805	−.0799	.8	Approximate zero lift.
	−.19	.162	.222	−.127	−.103	23.3	Approximate N. D. condition.
10	1.49	.223	.361	.421	.434	−3.0	H. A. A. condition.
	1.44	.223	.361	.403	.382	−5.5	H. A. A. condition.
	.02	.223	.361	−.110	−.120	−8.3	Approximate zero lift.
	−.19	.223	.361	−.186	−.153	21.6	Approximate N. D. condition.
15	1.49	.252	.477	.579	.589	−1.7	H. A. A. condition.
	1.44	.252	.477	.555	.529	4.9	H. A. A. condition.
	.02	.252	.477	−.123	−.137	−10.2	Approximate zero lift.
	−.19	.252	.477	−.223	−.190	17.4	Approximate N. D. condition.
20	1.49	.236	.571	.727	.723	.6	H. A. A. condition.
	1.44	.236	.571	.698	.657	6.2	H. A. A. condition.
	.02	.236	.571	−.112	−.140	−20.0	Approximate zero lift.
	−.19	.236	.571	−.232	−.224	3.6	Approximate N. D. condition.

N. A. C. A. 84 AIRFOIL

Maximum mean camber=5.25% c; C_B=0.762

Spar location (% c)	C_L	K_1 (from curve)	K_2 (from curve)	C_S Computed	C_S Experimental	Error, %	Remarks
5	1.51	0.162	0.222	0.212	0.216	−1.9	H. A. A. condition.
	1.37	.162	.222	.181	.180	.6	H. A. A. condition.
	0	.162	.222	−.123	−.120	2.5	Zero lift.
	−.19	.162	.222	−.166	−.159	4.4	Approximate N. D. condition.
10	1.51	.223	.361	.375	.396	−5.3	H. A. A. condition.
	1.37	.223	.361	.325	.336	−3.3	H. A. A. condition.
	0	.223	.361	−.170	−.181	−6.1	Zero lift.
	−.19	.223	.361	−.239	−.239	0	Approximate N. D. condition.
15	1.51	.252	.477	.528	.539	−2.0	H. A. A. condition.
	1.37	.252	.477	.462	.466	−.9	H. A. A. condition.
	0	.252	.477	−.192	−.206	−6.8	Zero lift.
	−.19	.252	.477	−.283	−.284	−.4	Approximate N. D. condition.
20	1.51	.236	.571	.682	.669	1.9	H. A. A. condition.
	1.37	.236	.571	.602	.585	2.9	H. A. A. condition.
	0	.236	.571	−.180	−.214	−15.9	Zero lift.
	−.19	.236	.571	−.289	−310	−6.8	Approximate N. D. condition.

TABLE I—Continued

COMPARISON OF SHEAR COEFFICIENTS FROM FORMULA AND FROM PRESSURE-DISTRIBUTIOM TESTS IN THE VARIABLE-DENSITY TUNNEL—Con.

N. A. C. A. 84–J AIRFOIL

Maximum mean camber=7.3% c; C_B=0.97

Spar location (% c)	C_L	K_1 (from curve)	K_2 (from curve)	C_S Computed	C_S Experimental	Error, %	Remarks
5	1.72	0.162	0.222	0.225	0.230	−2.2	H. A. A. condition.
	1.63	.162	.222	.205	.188	9.0	H. A. A. condition.
	0	.162	.222	−.157	−.163	−3.7	Zero lift.
	−.16	.162	.222	−.193	−.121	59.5	Approximate N. D. condition.
10	1.72	.223	.361	.405	.410	−1.2	H. A. A. condition.
	1.63	.223	.361	.372	.350	6.3	H. A. A. condition.
	0	.223	.361	−.216	−.242	−10.7	Zero lift.
	−.16	.223	.361	−.274	−.206	33.0	Approximate N. D. condition.
15	1.72	.252	.477	.576	.564	2.1	H. A. A. condition.
	1.63	.252	.477	.533	.488	9.2	H. A. A. condition.
	0	.252	.477	−.244	−.286	−14.7	Zero lift.
	−.16	.252	.477	−.321	−.256	25.4	Approximate N. D. condition.
20	1.72	.236	.571	.753	.713	5.6	H. A. A. condition.
	1.63	.236	.571	.702	.622	12.9	H. A. A. condition.
	0	.236	.571	−.229	−.310	−26.1	Zero lift.
	−.16	.236	.571	−.320	−.288	11.1	Approximate N. D. condition.

TABLE II

COMPARISON OF LEADING-EDGE LOADS AS COMPUTED, TO THOSE LOADS OBTAINED IN ACTUAL FLIGHT

CLARK Y AIRFOIL (UPPER WING DOUGLAS M–3)

Maximum mean camber 3.6% c; C_B=0.525; Chord 5.667 feet

Spar location (%c)	C_{NP}	K_1 (from curve)	K_2 (from curve)	Speed f. p. s.	$w_{l.e.}$ (Computed)	$w_{l.e.}$ (Experimental)	Error, %	Remarks
7.2	1.533	0.191	0.285	107.6	26.3	29.6	−11.0	H. A. A. condition.
	.0144	.191	.285	128.0	10.6	9.6	10.5	
	−.2344	.191	.285	122.5	16.9	16.0	5.6	

GÖTTINGEN 436 AIRFOIL (UPPER WING BOEING PW–9)

Maximum mean camber 3.55% c; C_B=0.515; Chord 5.42 feet

15	1.743	0.252	0.477	144	93.7	103.6	−9.6	H. A. A. condition.
	1.649	.252	.477	214	193.7	202.0	−4.1	H. A. A. condition.
	1.682	.252	.477	183	145.1	161.7	−10.3	H. A. A. condition.
	1.810	.252	.477	180	153.1	165.3	−7.4	H. A. A. condition.
	1.660	.252	.477	212	191.7	203.0	−5.6	H. A. A. condition.
	.0564	.252	.477	360	−86.0	−73.2	17.5	Approximate zero lift.
	−.3466	.252	.477	211	−84.6	−85.6	−1.2	
	−.4313	.252	.477	207	−92.8	−92.8	0	
	−.3668	.252	.477	205	−82.6	−83.6	1.2	
	−.3795	.252	.477	212	−90.1	−89.6	.6	
	.0401	.252	.477	381	−103.8	−107.0	−3.0	

GÖTTINGEN 436 AIRFOIL (LOWER WING BOEING PW–9)

Maximum mean camb er 3.55% c; C_B=0.515; Chord 4.23 feet

12.2	1.298	0.2405	0.415	144	43.3	45.6	−5.0	H. A. A. condition.
	1.194	.2405	.415	214	85.7	87.2	−1.7	H. A. A. condition.
	1.257	.2405	.415	183	67.1	70.4	−4.7	H. A. A. condition.
	1.324	.2405	.415	180	69.3	72.8	−4.8	H. A. A. condition.
	1.207	.2405	.415	212	85.2	85.4	−.2	H. A. A. condition.
	.0403	.2405	.415	360	−69.8	−117.0	−40.3	Approximate zero lift.
	−.314	.2405	.415	211	−56.9	−76.0	−25.1	
	−.358	.2405	.415	207	−58.9	−76.8	−23.3	
	−.291	.2405	.415	205	−51.8	−63.2	−18.0	
	−.313	.2405	.415	212	−57.4	−72.0	−20.3	
	.0378	.2405	.415	366	−72.8	−100.0	−27.2	
	.087	.2405	.415	367	−59.7	−84.0	−28.9	
	.0997	.2405	.415	370	−57.2	−81.2	−29.6	
	.0913	.2405	.415	363	−57.0	−78.0	−26.9	
	.130	.2405	.415	361	−45.9	−66.5	−31.0	

U. S. GOVERNMENT PRINTING OFFICE: 1932

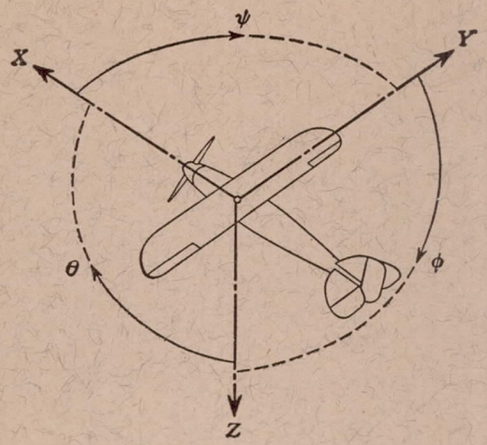

Positive directions of axes and angles (forces and moments) are shown by arrows

Axis		Force (parallel to axis) symbol	Moment about axis			Angle		Velocities	
Designation	Symbol		Designation	Symbol	Positive direction	Designation	Symbol	Linear (component along axis)	Angular
Longitudinal	X	X	rolling	L	$Y \longrightarrow Z$	roll	ϕ	u	p
Lateral	Y	Y	pitching	M	$Z \longrightarrow X$	pitch	θ	v	q
Normal	Z	Z	yawing	N	$X \longrightarrow Y$	yaw	ψ	w	r

Absolute coefficients of moment

$$C_l = \frac{L}{qbS} \qquad C_m = \frac{M}{qcS} \qquad C_n = \frac{N}{qbS}$$

Angle of set of control surface (relative to neutral position), δ. (Indicate surface by proper subscript.)

4. PROPELLER SYMBOLS

D, Diameter.

p, Geometric pitch.

p/D, Pitch ratio.

V', Inflow velocity.

V_s, Slipstream velocity.

T, Thrust, absolute coefficient $C_T = \frac{T}{\rho n^2 D^4}$

Q, Torque, absolute coefficient $C_Q = \frac{Q}{\rho n^2 D^5}$

P, Power, absolute coefficient $C_P = \frac{P}{\rho n^3 D^5}$.

C_s, Speed power coefficient $= \sqrt[5]{\frac{\rho V^5}{P n^2}}$.

η, Efficiency.

n, Revolutions per second, r. p. s.

Φ, Effective helix angle $= \tan^{-1}\left(\frac{V}{2\pi r n}\right)$

5. NUMERICAL RELATIONS

1 hp = 76.04 kg/m/s = 550 lb./ft./sec.
1 kg/m/s = 0.01315 hp
1 mi./hr. = 0.44704 m/s
1 m/s = 2.23693 mi./hr.

1 lb. = 0.4535924277 kg.
1 kg = 2.2046224 lb.
1 mi. = 1609.35 m = 5280 ft.
1 m = 3.2808333 ft.